PRINCETON UNIVERSITY

FRONTERA

AST20010

Kinetic simulations of transport and turbulence in collisionless astrophysical plasmas

Himawan Winarto

on behalf of

Matthew Kunz (PI), Lev Arzamasskiy, Archie Bott, Alisa Galishnikova, Zach Hemler, David Hosking, Phillipp Kempski, Stephen Majeski, Eliot Quataert, Alex Schekochihin, Jonathan Squire, Himawan Winarto, Evan Yerger, Michael Zhang, Muni Zhou

Our group uses kinetic and MHD simulations to study turbulence, transport, and thermodynamics in space/astrophysical plasmas

Matthew Kunz

Lev Arzamasskiy

Archie Bott

Alisa Galishnikova

Zach Hemler

David Hosking

Phillipp Kempski

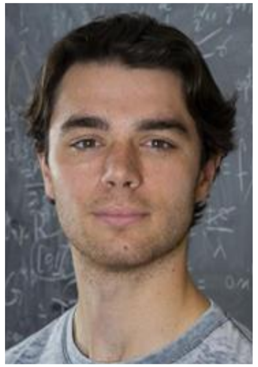

Stephen Majeski

Eliot Quataert

Alex Schekochihin

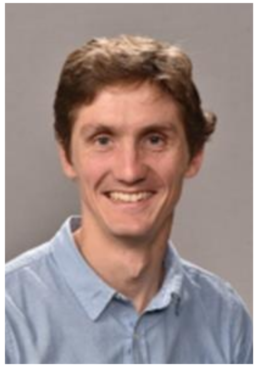

Jono Squire

Himawan Winarto

Evan Yerger

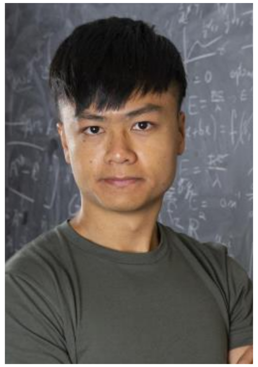

Michael Zhang

Muni Zhou

Astrophysical systems can be dilute and hot

$$n \sim 3 \times 10^{-3}\ \mathrm{cm}^{-3}$$

$$T \sim 8\ \mathrm{keV}$$

$$B \sim 5\ \mu\mathrm{G}$$

$$\beta \sim 10^{2}$$

Ratio of thermal to magnetic pressure

[Bonafede+, 2010]

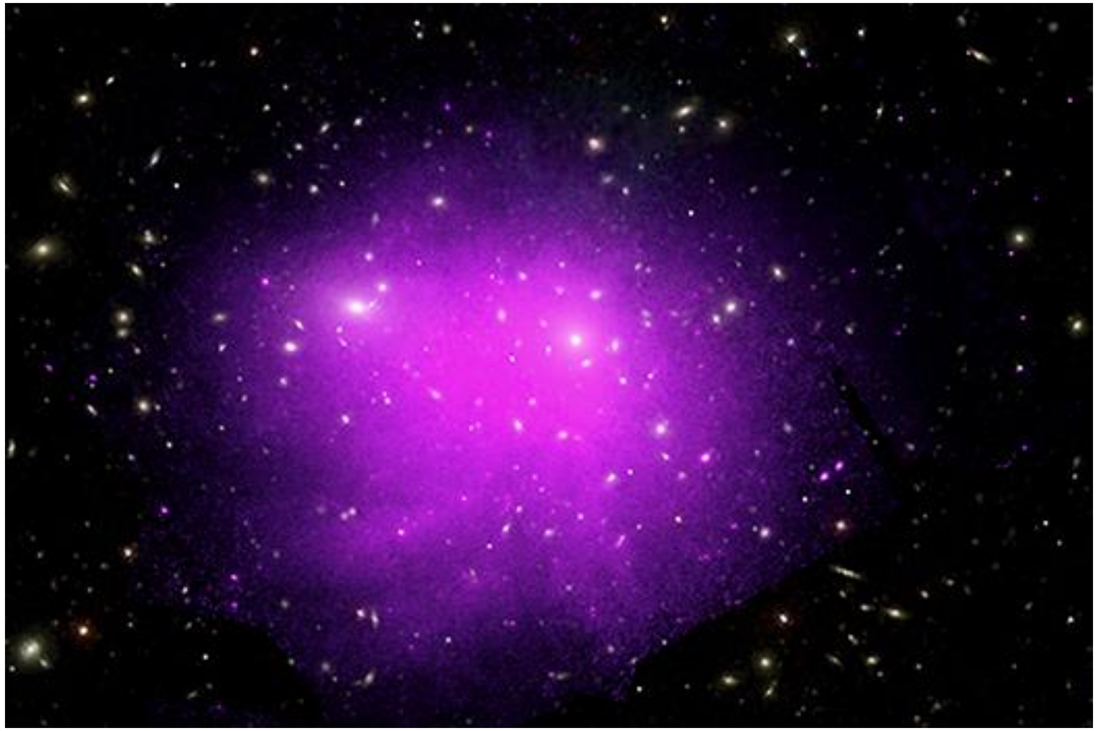

Coma cluster [Zhuravleva+ 2019]

Astrophysical systems can be dilute and hot

$$\beta \sim 10^2$$

$$L \sim 100 \text{ kpc}$$

$$\lambda_{\text{mfp}} \sim 10 \text{ kpc}$$

$$\rho_i \sim 1 \text{ npc}$$

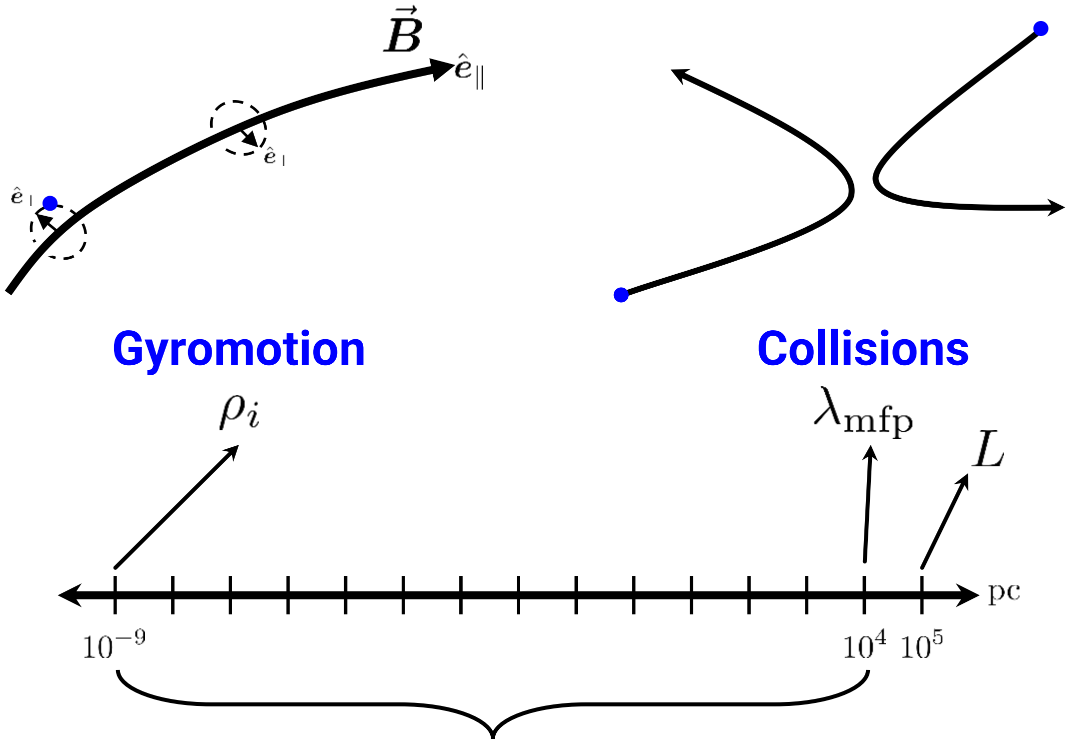

Orders of magnitude separation between microphysics and collisions

Similar scale separations in other collisionless systems

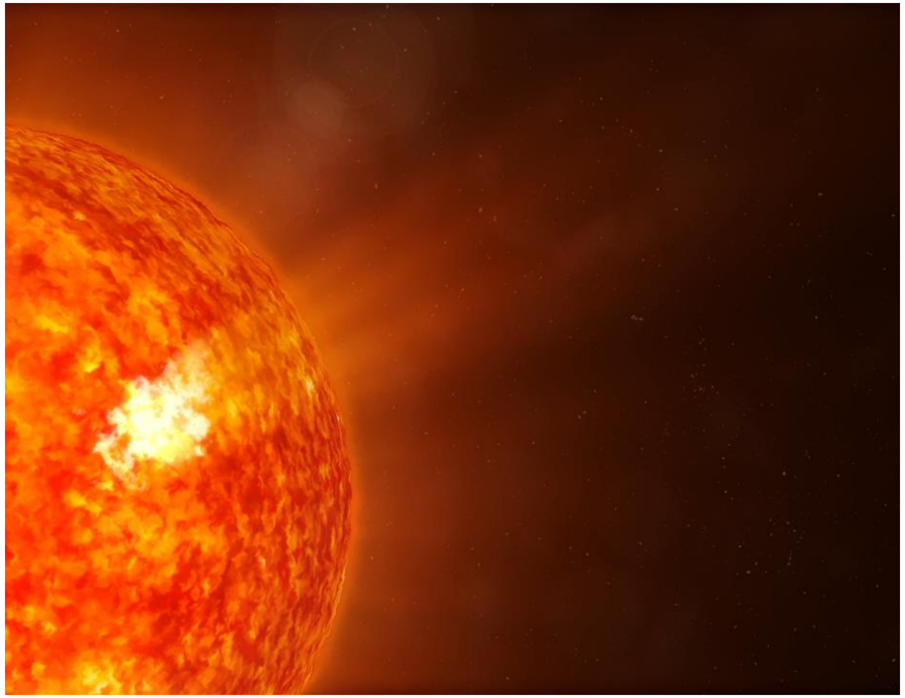

Solar Wind

$$\beta \gtrsim 1$$

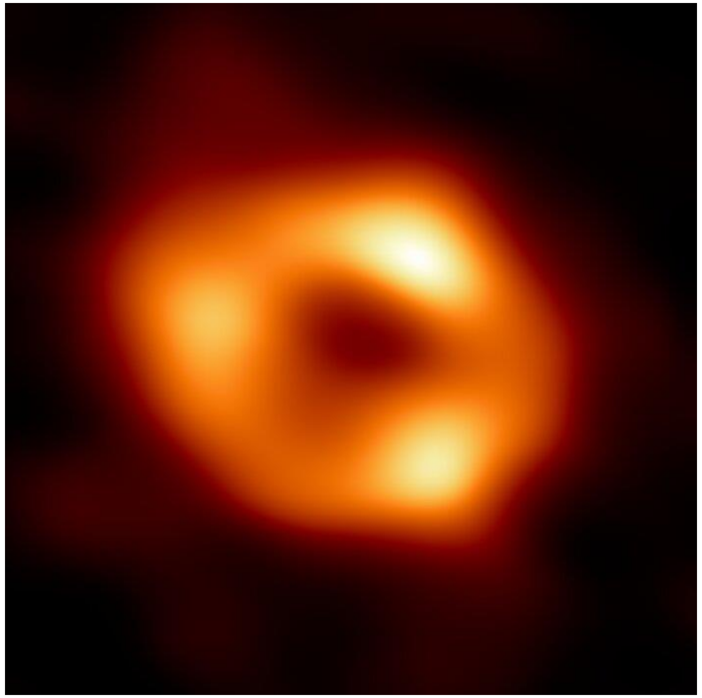

Black Hole Accretion

$$\beta \sim 10^1 - 10^2$$

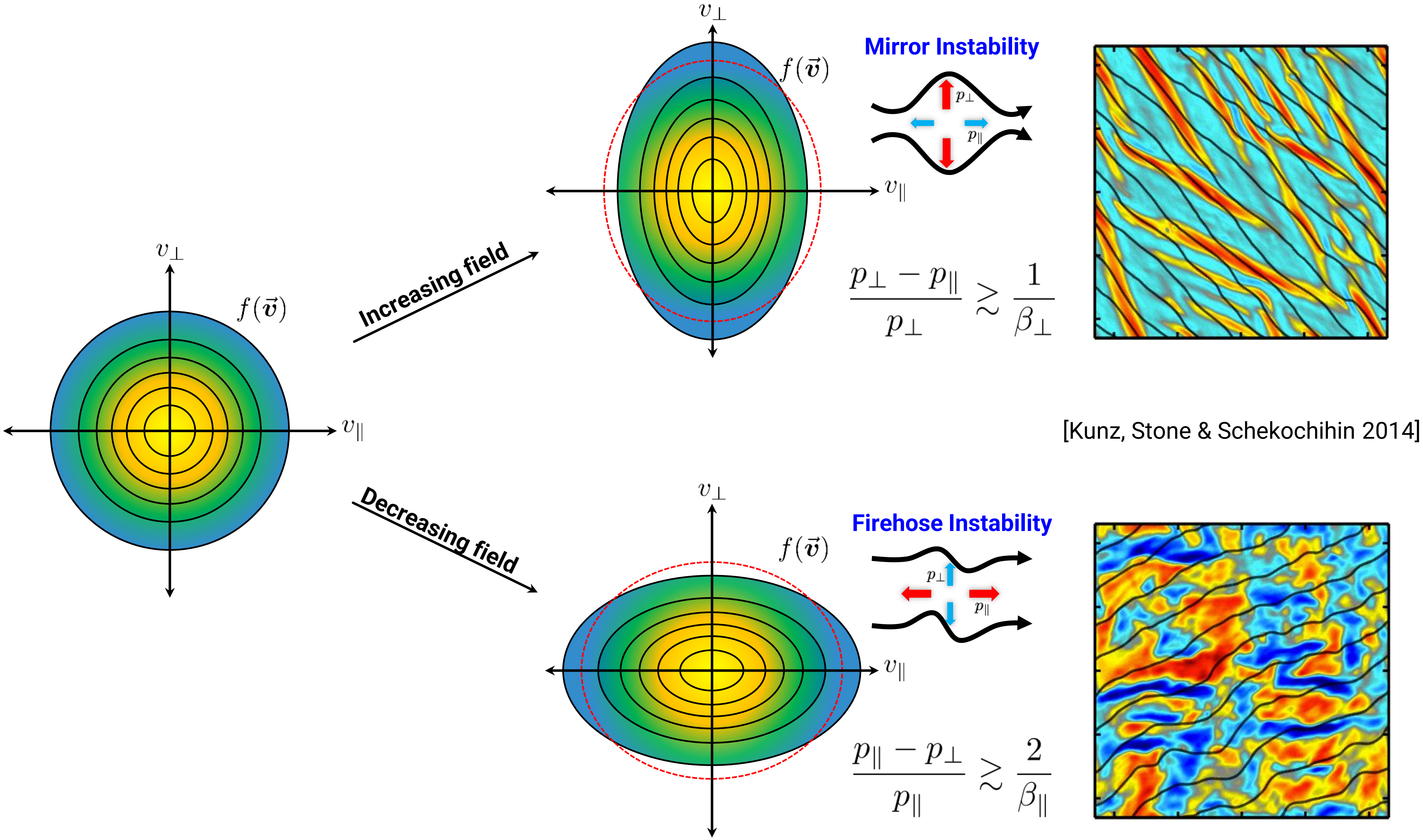
$v_\perp$
$f(\vec{v})$
$v_\parallel$
Increasing field
Decreasing field
Mirror Instability
$p_\perp$
$p_\parallel$
$\frac{p_\perp - p_\parallel}{p_\perp} \gtrsim \frac{1}{\beta_\perp}$
Firehose Instability
$\frac{p_\parallel - p_\perp}{p_\parallel} \gtrsim \frac{2}{\beta_\parallel}$
[Kunz, Stone & Schekochihin 2014]

Our group's papers using Frontera

- Collisionless conduction in a high-beta plasma: a collision operator for whistler turbulence
  Yerger, E. L., Kunz, M. W., Bott, A. F. A., and Spitkovsky, A., *in press* (2024).
- Magnetogenesis in a Collisionless Plasma: From Weibel Instability to Turbulent Dynamo
  Zhou, M., Zhdankin, V., Kunz, M. W., Loureiro, N. F., and Uzdensky, D. A., *ApJ* (2024).
- Cosmic ray transport in large-amplitude turbulence with small-scale field reversals
  Kempski, P. et al., *MNRAS* (2023).
- Electron-Ion Heating Partition in Imbalanced Solar-wind Turbulence
  Squire, J., Meyrand, R., and Kunz, M. W., *ApJ* (2023).
- Microphysically modified magnetosonic modes in collisionless, high-β plasmas
  Majeski, S., Kunz, M. W., and Squire, J., *JPP* (2023).
- Tearing Instability and Current-Sheet Disruption in the Turbulent Dynamo
  Galishnikova, A. K., Kunz, M. W., and Schekochihin, A. A., *PRX* (2022).
- High-frequency heating of the solar wind triggered by low-frequency turbulence
  Squire, J., Meyrand, R., Kunz, M. W., Arzamasskiy, L., Schekochihin, A. A., and Quataert, E., *Nature Astronomy* (2022).
- Triggering tearing in a forming current sheet with the mirror instability
  Winarto, H. W. and Kunz, M. W., *JPP* (2022).

Particle-In-Cell (PIC) Simulations

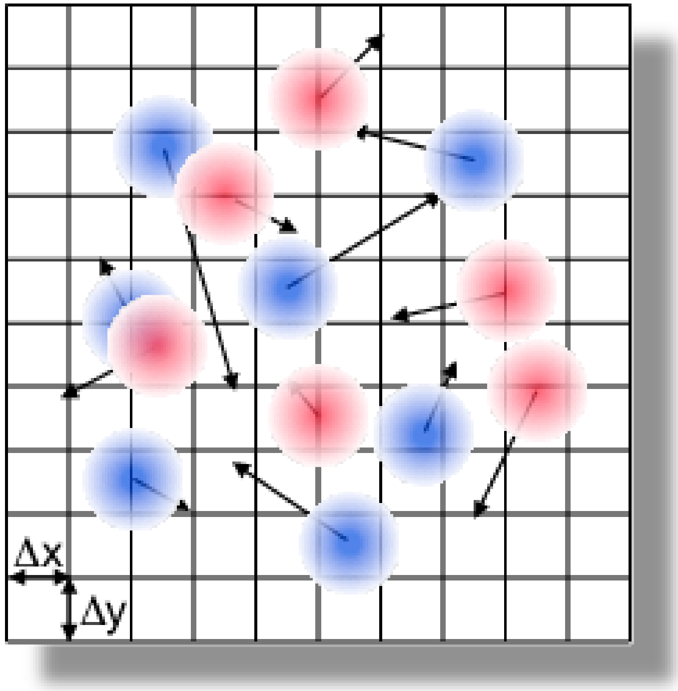

PIC illustration
[WarpX group]

Macroparticles are pushed by the electromagnetic forces…

$$\frac{\mathrm{d}\vec{\boldsymbol{x}}_p}{\mathrm{d}t} = \vec{\boldsymbol{v}}_p$$

$$\frac{\mathrm{d}\vec{\boldsymbol{v}}_p}{\mathrm{d}t} = \frac{q_s}{m_s}\left(\vec{\boldsymbol{E}} + \frac{\vec{\boldsymbol{v}}_p}{c} \times \vec{\boldsymbol{B}}\right)$$

…and deposited back to the grid to change the electromagnetic fields.

$$\boldsymbol{\nabla} \cdot \vec{\boldsymbol{E}} = 4\pi\rho \qquad \boldsymbol{\nabla} \times \vec{\boldsymbol{E}} = -\frac{1}{c}\frac{\partial \vec{\boldsymbol{B}}}{\partial t}$$

$$\boldsymbol{\nabla} \cdot \vec{\boldsymbol{B}} = 0 \qquad \boldsymbol{\nabla} \times \vec{\boldsymbol{B}} = \frac{4\pi}{c}\vec{\boldsymbol{J}} + \frac{1}{c}\frac{\partial \vec{\boldsymbol{E}}}{\partial t}$$

Our group mostly use the modified version of **TRISTAN-MP**.

Hybrid Simulations

Instead of evolving both electrons and ions as particles,
we can instead treat the electrons as a **neutralizing massless fluid**.

$$\forall \text{cell} : n_e = n_i$$

Current implementation in our hybrid-kinetic code **`PEGASUS++`**
enables our group to do large scale simulations with kinetic-ion effects.

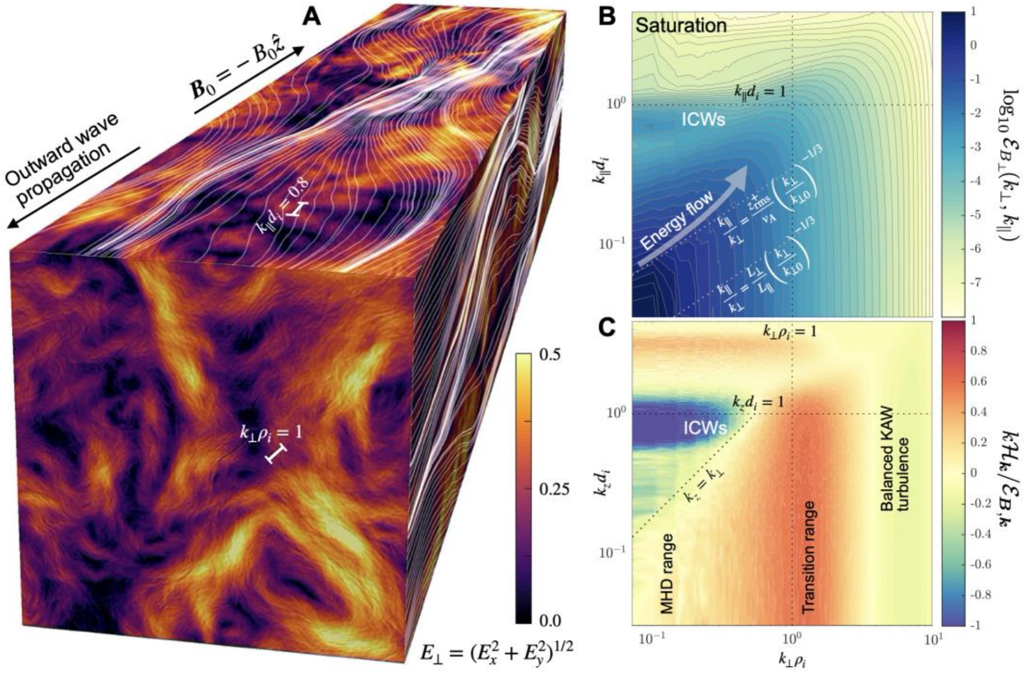

Helicity barrier

High-frequency heating of the solar wind
triggered by low-frequency turbulence
Squire *et al.* (2022)

Only balanced portion of Alfvenic cascade can
go through the ion-Larmor scale (barrier).

What cannot be captured by fluid models?

Collisionless conduction in a high-beta plasma: a collision operator for whistler turbulence

Yerger, E. L., Kunz, M. W., Bott, A. F. A., and Spitkovsky, A., *in press* (2024)

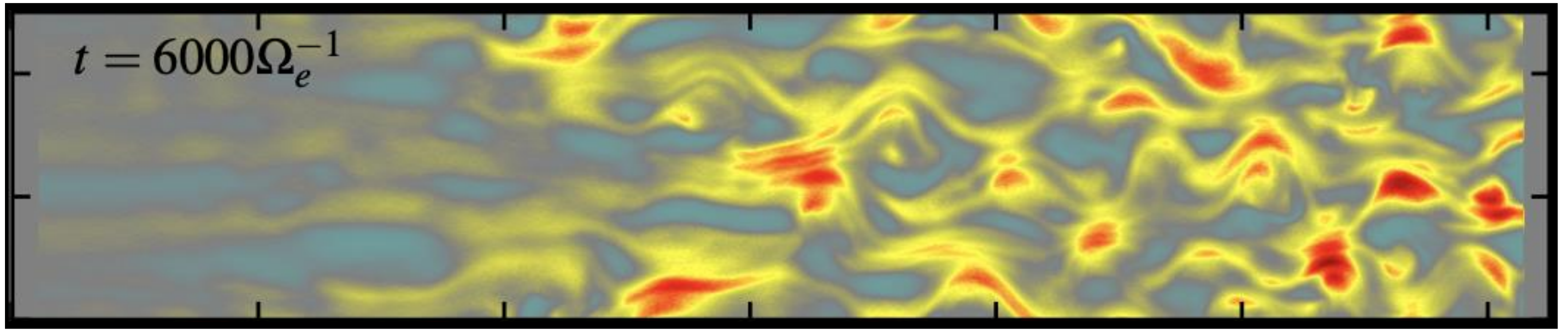

Heat flux excites **whistler instability** creating magnetic fluctuations that eventually regulates heat flux.

$$\nu_e \sim \beta_e \left| \frac{v_{\mathrm{th},e}}{L_T} \right| \quad \rightarrow \quad q_{\|,e} \sim \frac{1}{\beta_e} n T_e v_{\mathrm{th},e}$$

This scaling has been implemented in the fluid Braginskii-MHD simulations [Berlok + 2021; Perrone+ 2024].

Also obtains the whistler “**collision operator**”.

Track Particle Buffer

One way to construct collision operator is by tracking large number of particles at a much finer time resolutions.

Compared to the fluid quantities, track particles are **not guaranteed to always be in the same process**.

Naively, you can pair every track particles with a unique file. Doing this through large number Frontera nodes can easily crash the filesystem from the *rapid I/O calls*.

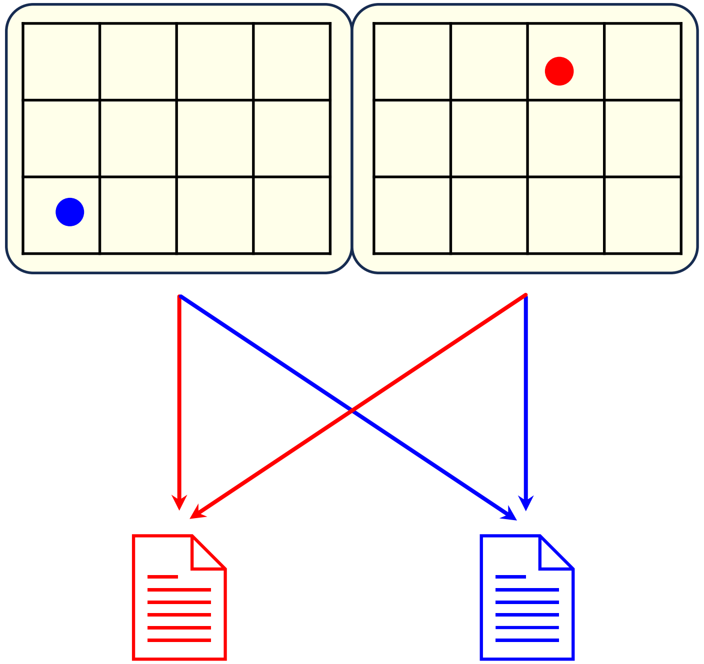

Track Particle Buffer

One way to construct collision operator is by tracking large number of particles at a much finer time resolutions.

Compared to the fluid quantities, track particles are **not guaranteed to always be in the same process**.

Naively, you can pair every track particles with a unique file. Doing this through large number Frontera nodes can easily crash the filesystem from the *rapid I/O calls*.

Implement a **local and main process buffers** for multiple high-frequency output, that are dumped at longer intervals.

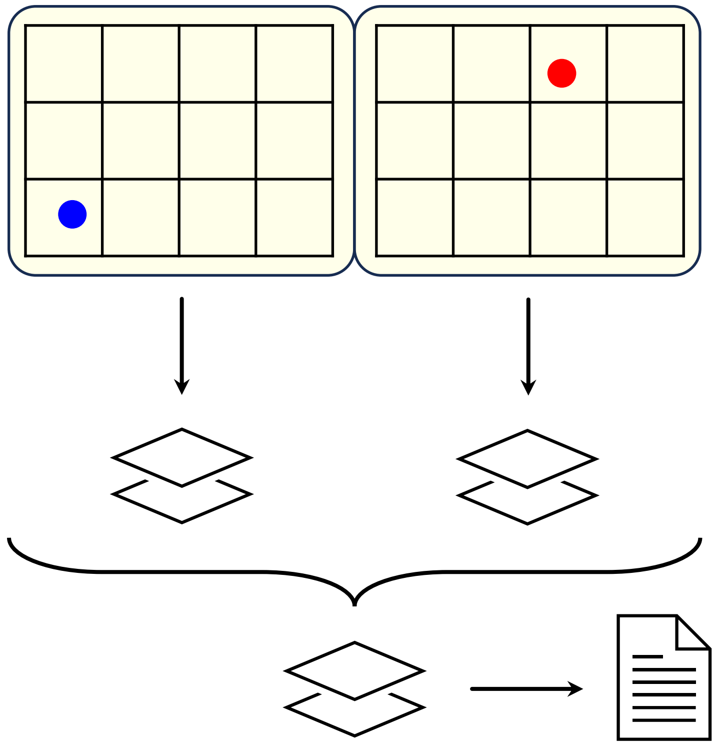

Expanding Box Simulations

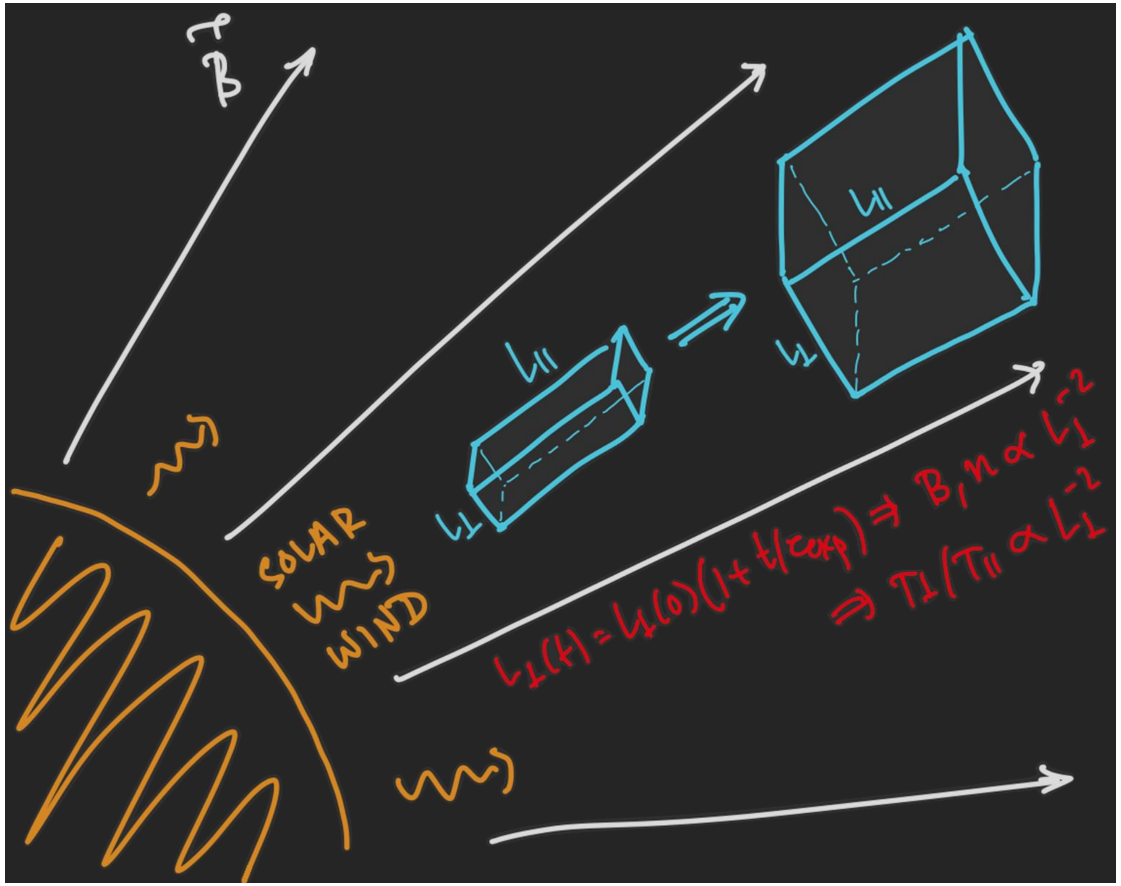

Expanding box simulations can better simulate the driving force of astrophysical systems.

Compression is modeled using continuous frame transformation that keeps **constant representation** in the code frame.

$$\mathbf{\Lambda}(t) \rightarrow \text{Expansion matrix}$$

$$\lambda(t) \equiv \det \mathbf{\Lambda}(t)$$

Current implementations in…

Pegasus++	**TRISTAN-MP**
$\vec{\boldsymbol{E}}' = \mathbf{\Lambda}\vec{\boldsymbol{E}}$	$\vec{\boldsymbol{E}}' = \lambda\mathbf{\Lambda}^{-1}\vec{\boldsymbol{E}}$
$\vec{\boldsymbol{B}}' = \lambda\mathbf{\Lambda}^{-1}\vec{\boldsymbol{B}}$	$\vec{\boldsymbol{B}}' = \lambda\mathbf{\Lambda}^{-1}\vec{\boldsymbol{B}}$
$n' \doteq \lambda n$	$n' = \lambda n$
$\vec{\boldsymbol{u}}' \doteq \mathbf{\Lambda}^{-1}\vec{\boldsymbol{u}}$	$\vec{\boldsymbol{u}}' = \mathbf{\Lambda}^{-1}\vec{\boldsymbol{u}}$

Expanding Box Simulations

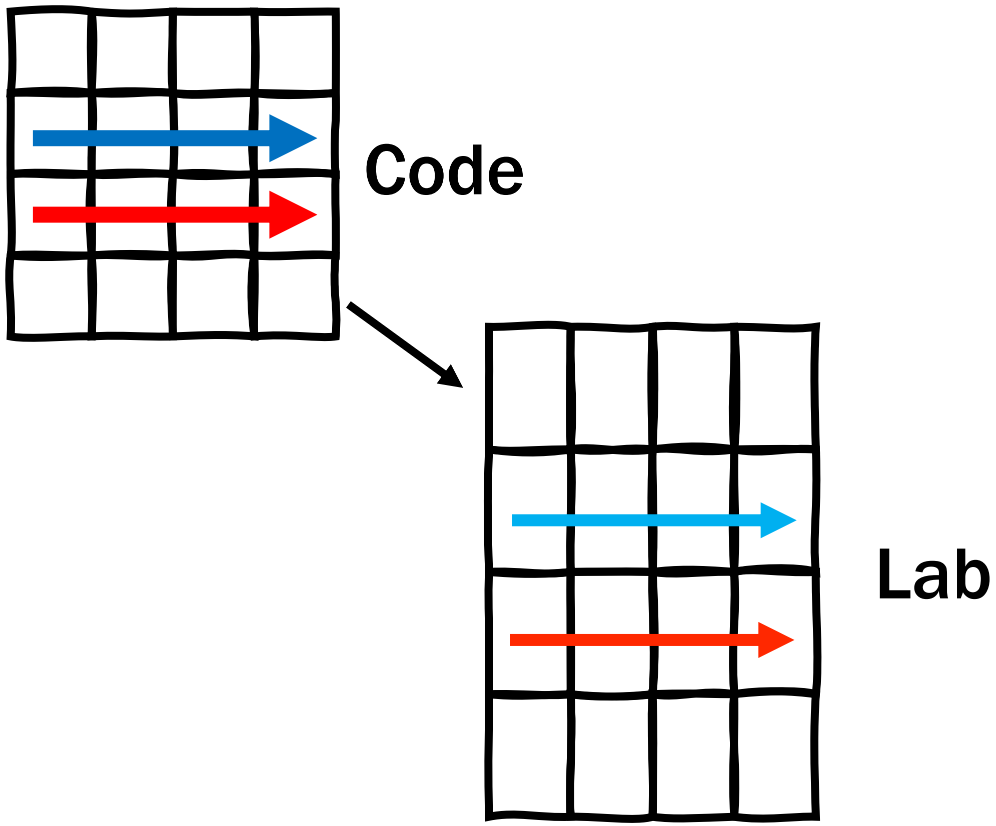

Expanding box simulations can better simulate the driving force of astrophysical systems.

Compression is modeled using continuous frame transformation that keeps **constant representation** in the code frame.

$$\boldsymbol{\Lambda}(t) \rightarrow \text{Expansion matrix}$$
$$\lambda(t) \equiv \det \boldsymbol{\Lambda}(t)$$

Current implementations in…

Pegasus++

$$\vec{\boldsymbol{E}}' = \boldsymbol{\Lambda}\vec{\boldsymbol{E}}$$
$$\vec{\boldsymbol{B}}' = \lambda\boldsymbol{\Lambda}^{-1}\vec{\boldsymbol{B}}$$
$$n' \doteq \lambda n$$
$$\vec{\boldsymbol{u}}' \doteq \boldsymbol{\Lambda}^{-1}\vec{\boldsymbol{u}}$$

TRISTAN-MP

$$\vec{\boldsymbol{E}}' = \lambda\boldsymbol{\Lambda}^{-1}\vec{\boldsymbol{E}}$$
$$\vec{\boldsymbol{B}}' = \lambda\boldsymbol{\Lambda}^{-1}\vec{\boldsymbol{B}}$$
$$n' = \lambda n$$
$$\vec{\boldsymbol{u}}' = \boldsymbol{\Lambda}^{-1}\vec{\boldsymbol{u}}$$

Collisionless resistivity of firehose-unstable plasma

Winarto, H. W. and Kunz, M. W., *in prep*

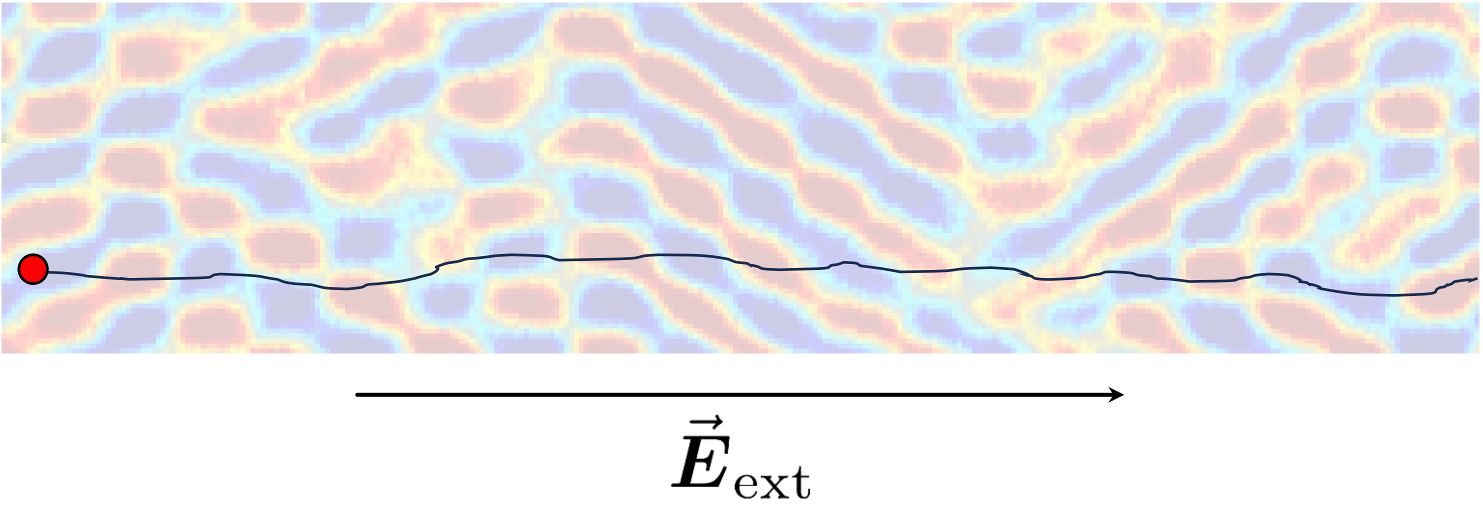

Persistent perturbations of firehose instability can scatter electrons and modify **electron currents**.

Resistivity sets the field reversal scale in turbulence-dynamo and rate of reconnection.

Collisionless resistivity of firehose-unstable plasma

Winarto, H. W. and Kunz, M. W., *in prep*

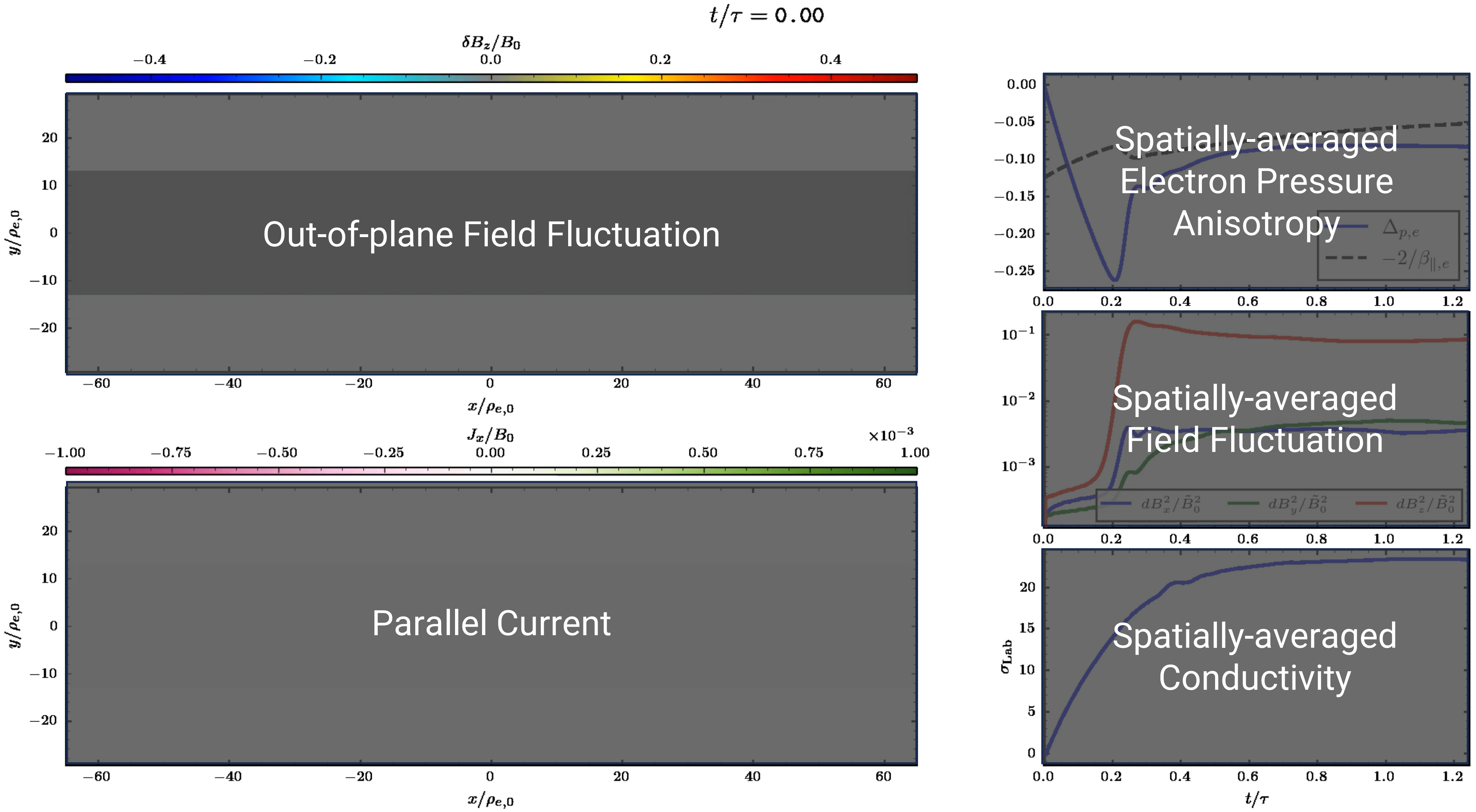

Triggering tearing in a forming current sheet with the mirror instability

Winarto, H. W. and Kunz, M. W., *JPP* (2022)

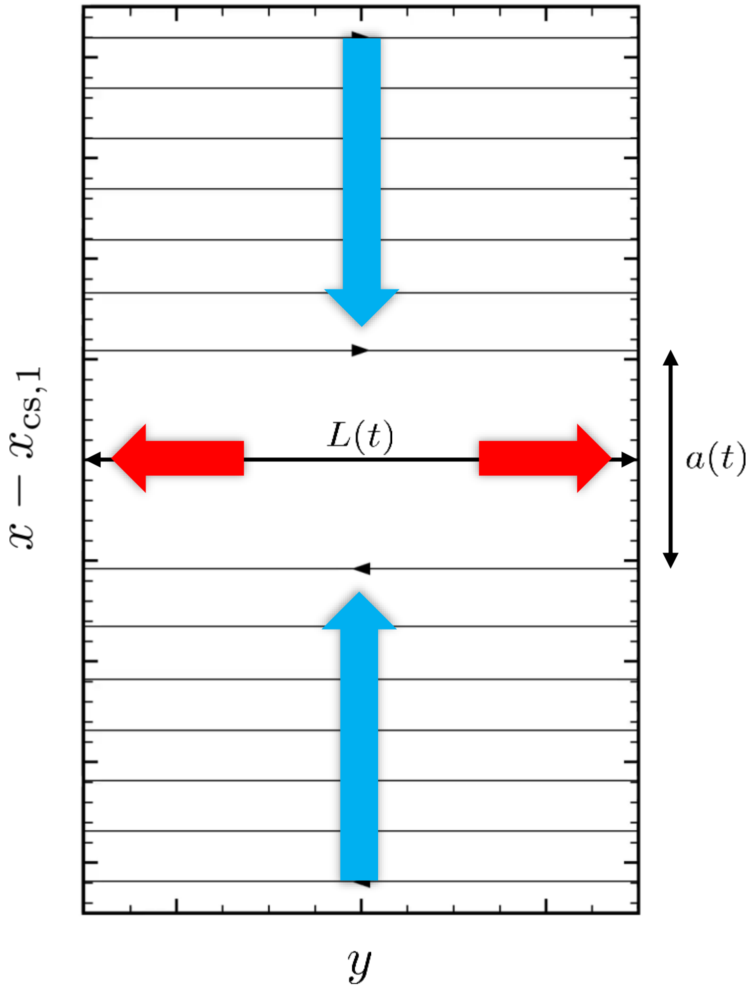

Consider a **thinning current sheet** in a collisionless, magnetized plasma.

Magnetic reconnection is a topological process that converts magnetic field energy to kinetic energy.

System will rapidly go mirror-unstable in high-beta collisionless plasma and can jump-start magnetic reconnection earlier than predicted from pure tearing modes.

Provides a natural explanation for recent laser-plasma experiments of driven reconnection with collisionless ions, which indicated an earlier onset of tearing having larger growth rates and significantly smaller scales than anticipated (Fox W. *et al.*, arXiv).

Triggering tearing in a forming current sheet with the mirror instability

Winarto, H. W. and Kunz, M. W., *JPP* (2022)

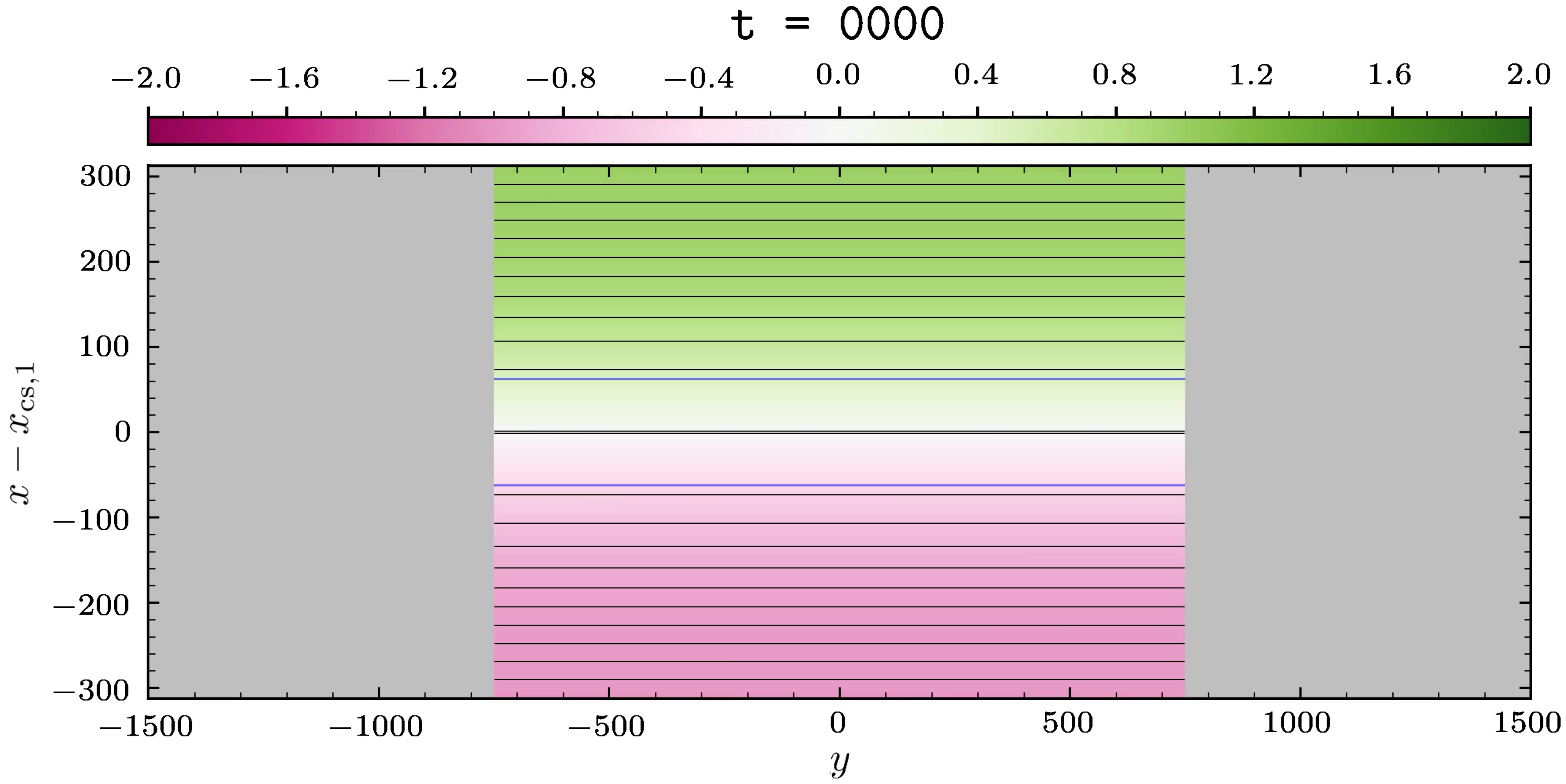

Minor-ion Heating in Solar Wind

Zhang et al. from Squire *et al., 2022*

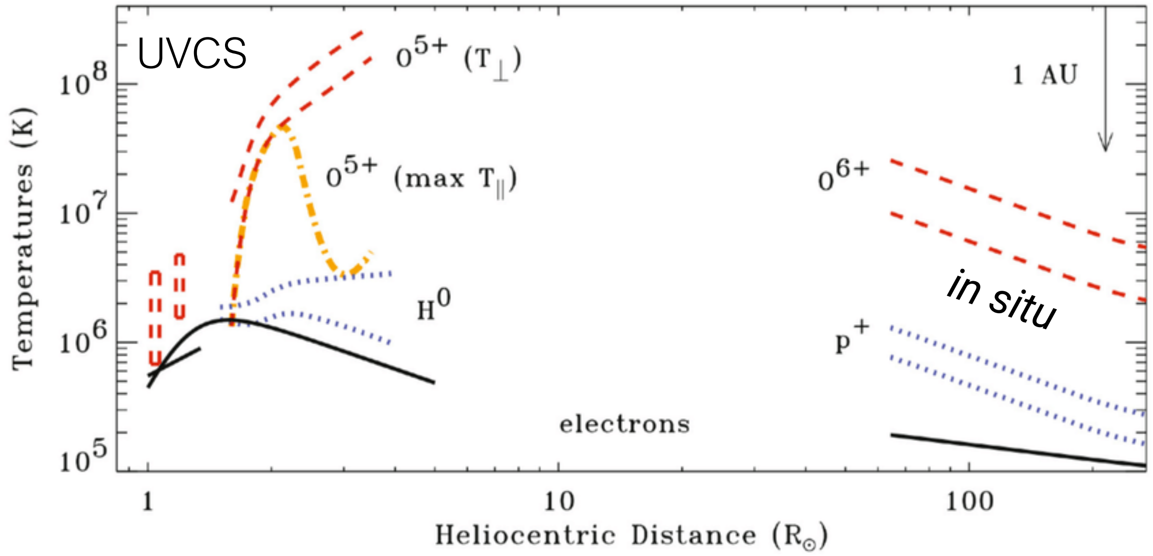

Minor ions are heated more strongly than protons in solar-wind.

Study focuses on how the heating mechanism differs from balanced and imbalanced turbulence.

Minor-ion Heating in Solar Wind

Zhang et al. from Squire *et al., 2022*

Proton velocity distribution function (VDF)

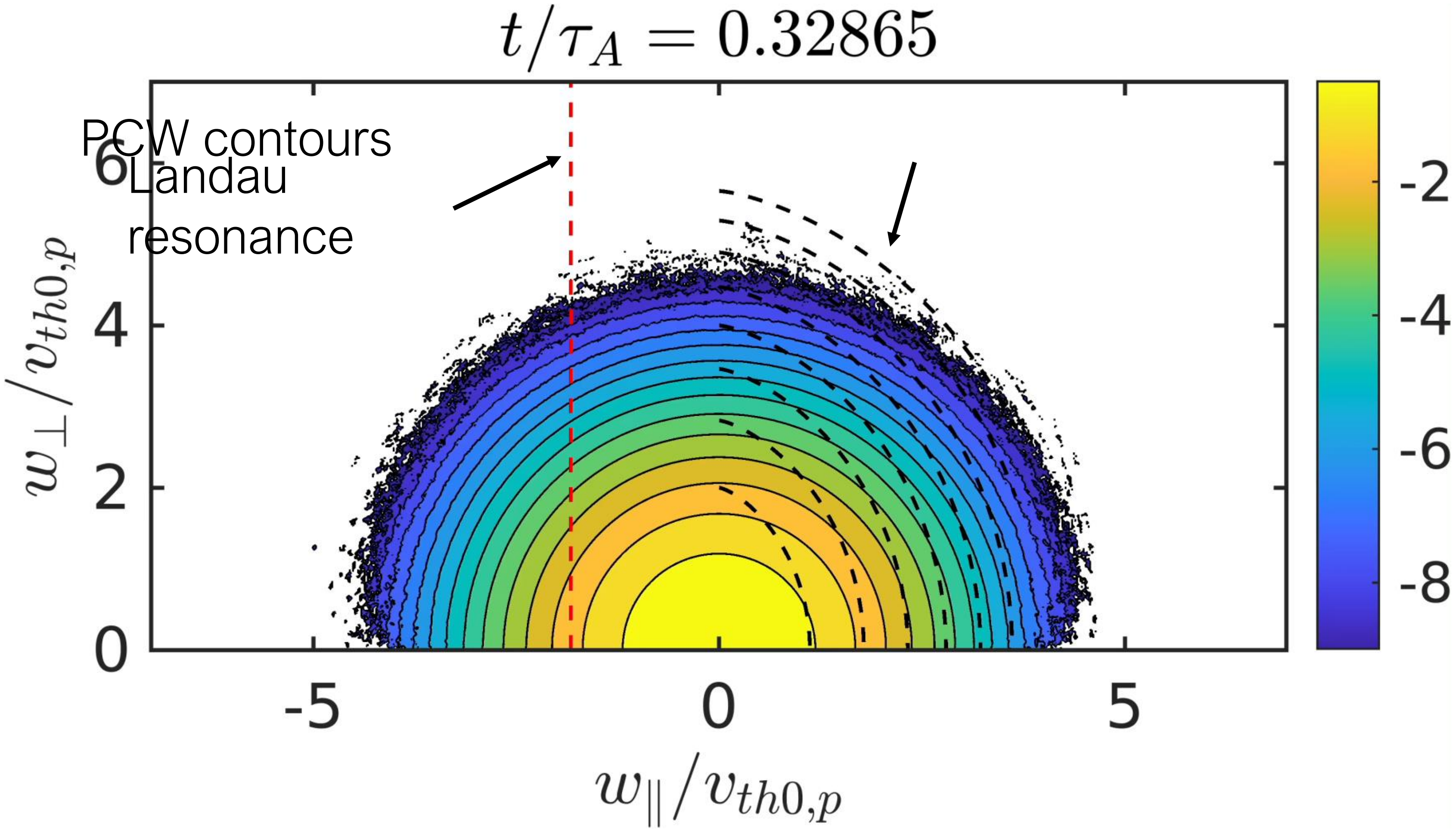

Minor-ion Heating in Solar Wind

Zhang et al. from Squire *et al.*, *2022*

He^{++} velocity distribution function (VDF)

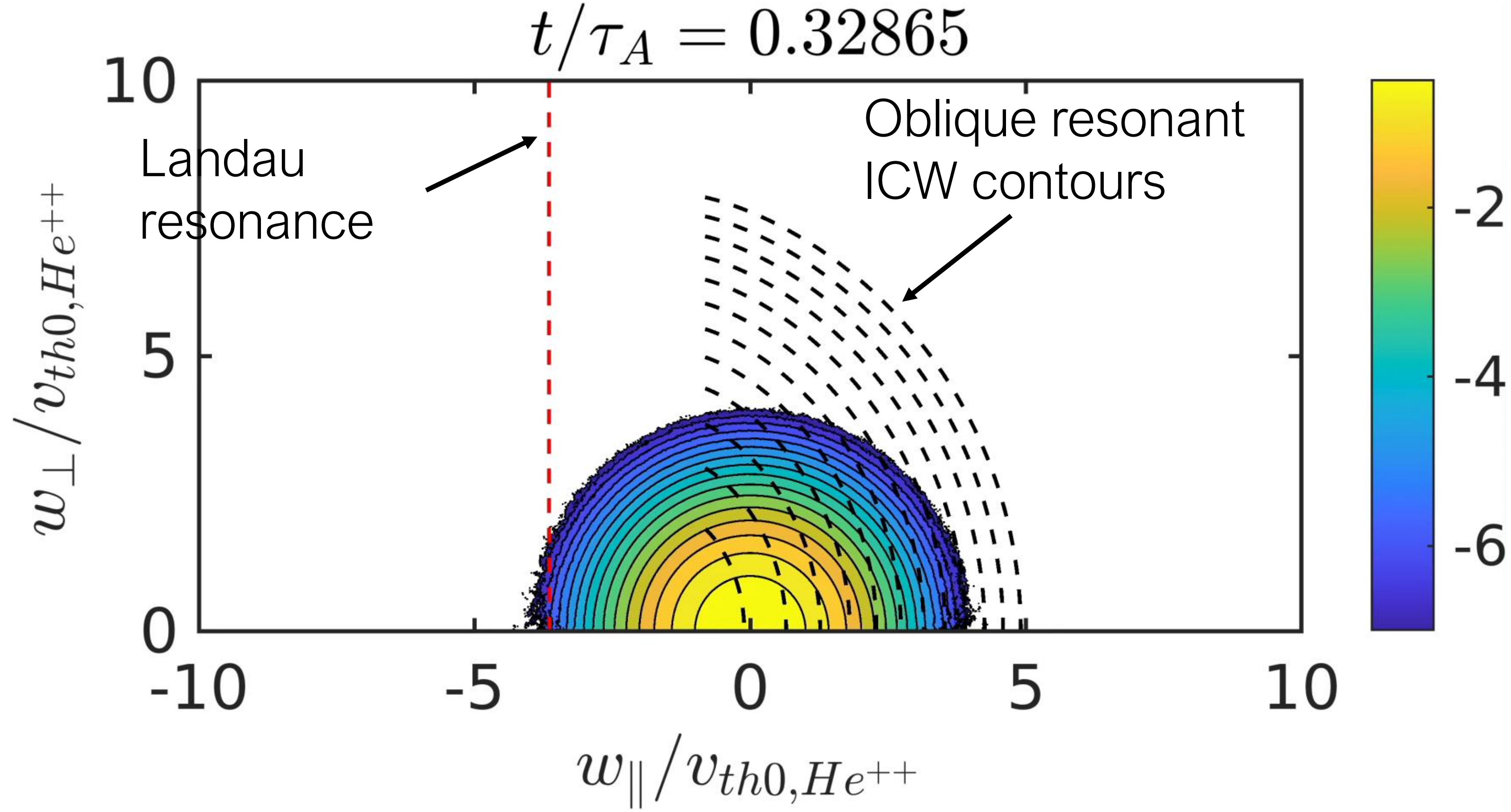

Tearing Instability and Current-Sheet Disruption in the Turbulent Dynamo

Galishnikova, A. K., Kunz, M. W., and Schekochihin, A. A., *PRX* (2022)

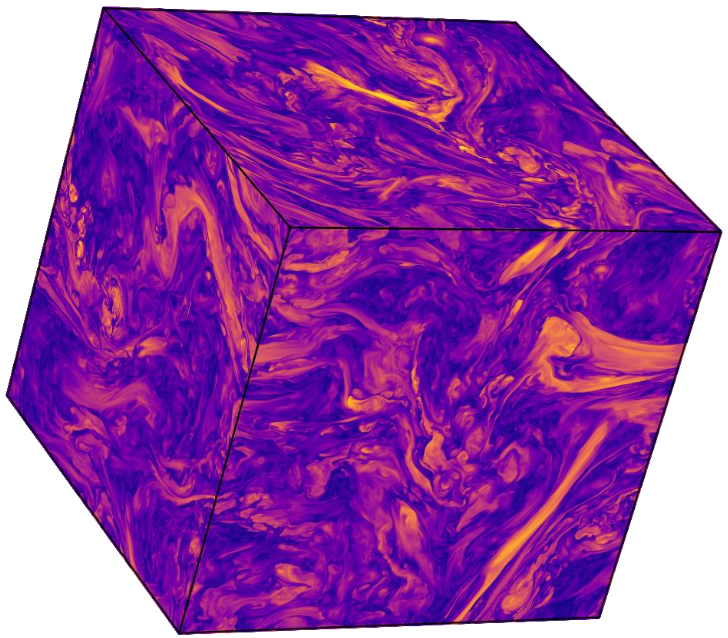

Elongated current sheets naturally produced by the turbulent dynamo become disrupted by **tearing instability** during the nonlinear stage of dynamo.

This changes the geometry and field spectrum by producing large-scale structures.

Taking the restart files from we can let the field lines relax.

Hemler Z. *et al.*

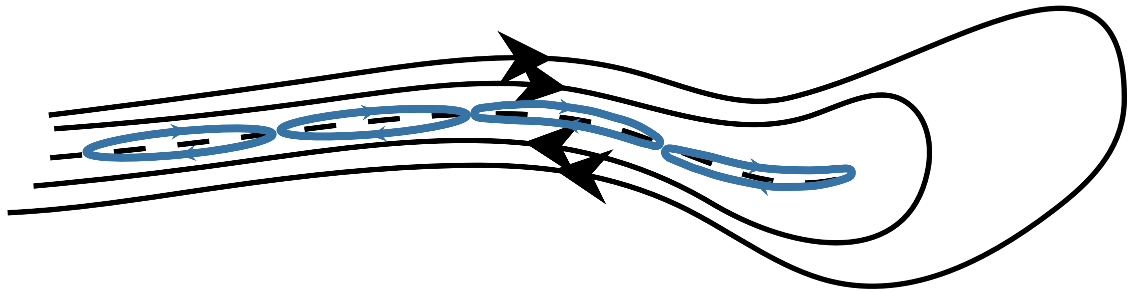

Decaying Dynamo

Hemler Z., Hosking D. & Kunz M.

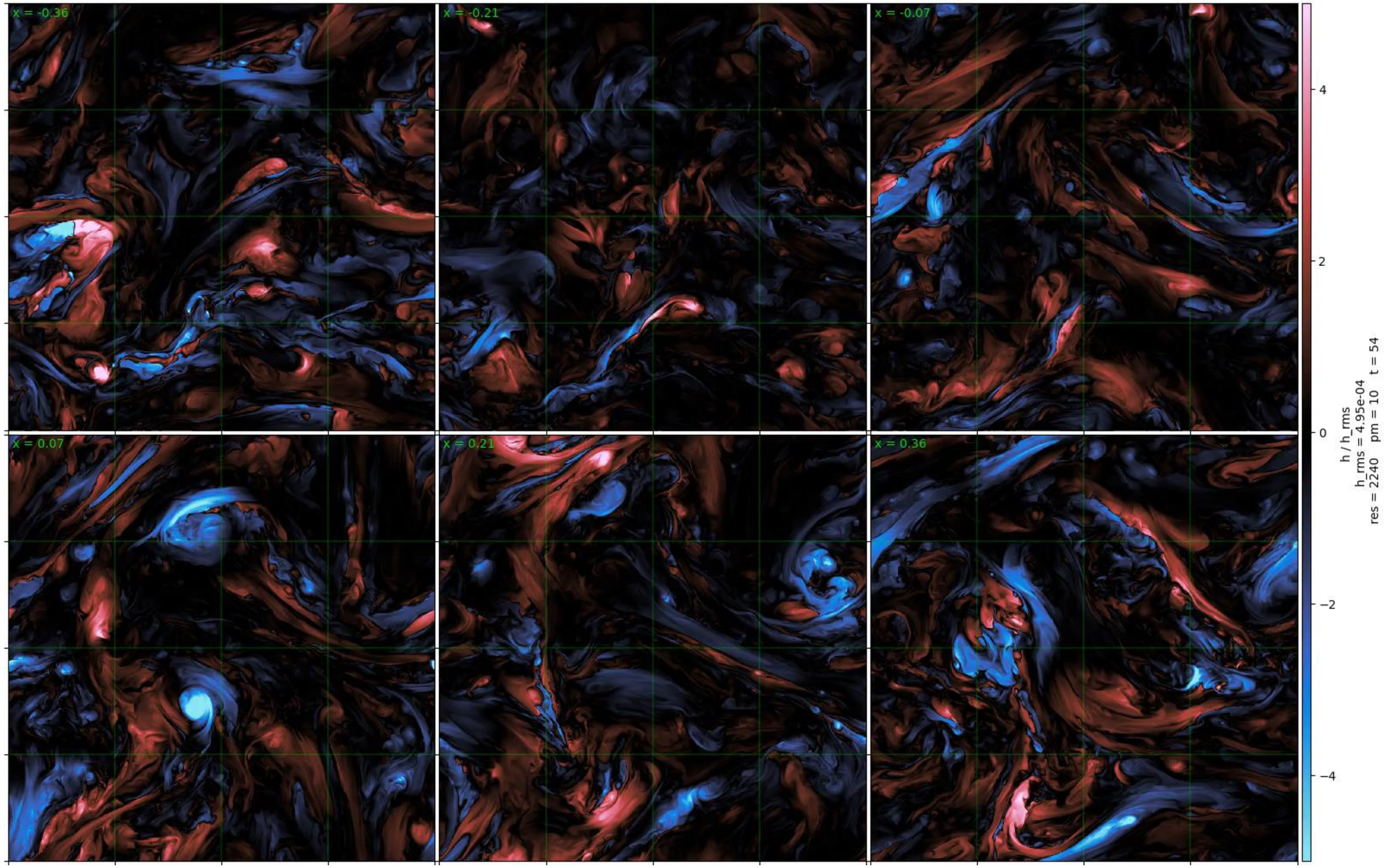

Magnetogenesis in a Collisionless Plasma: From Weibel Instability to Turbulent Dynamo

Zhou, M., Zhdankin, V., Kunz, M. W., Loureiro, N. F., and Uzdensky, D. A., ApJ (2024)

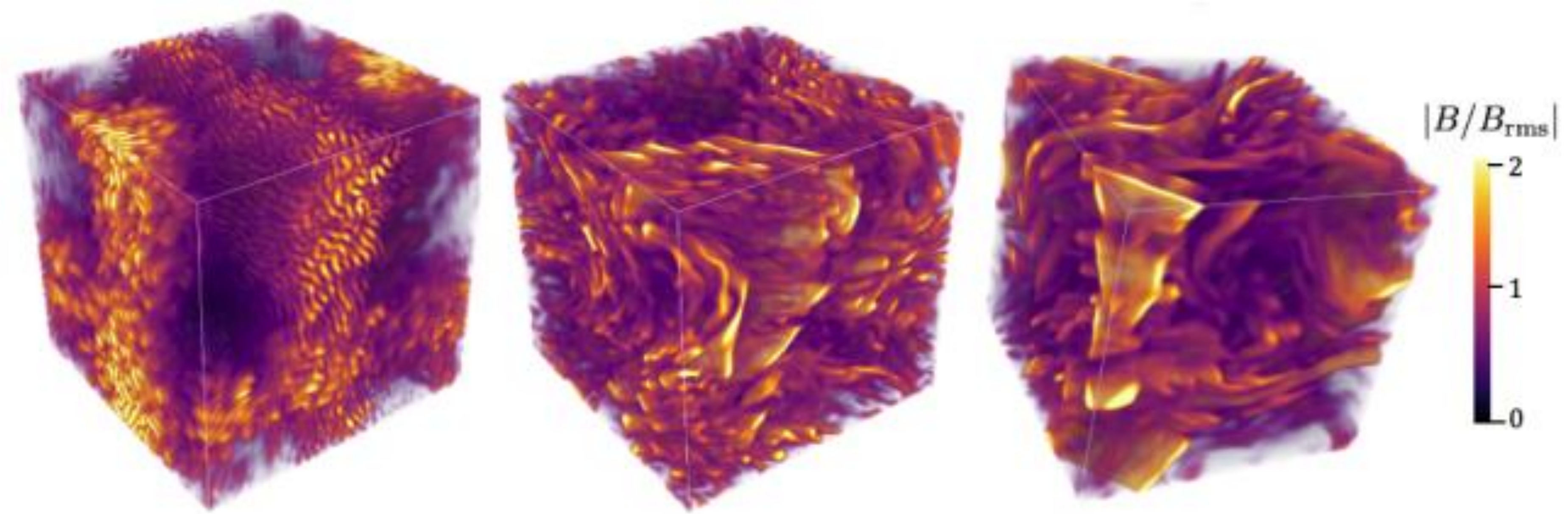

Using a fully kinetic PIC simulation, limited to electron-positron plasma we can see how magnetic fields are cascading into larger scales from the Weibel seeds.

Upcoming run for hybrid dynamo, updating previous work by St-Onge & Kunz (2018).

Extra Slides

Change in magnetic field can create pressure anisotropy…

$$\frac{p_\perp}{nB} \sim \text{const}$$

$$\frac{p_\parallel B^2}{n^3} \sim \text{const}$$

Collision rate sets the size of anisotropy

[Braginskii+, 1965]

$$\frac{p_\perp - p_\parallel}{p} \sim \frac{1}{\nu_{ii}} \frac{\mathrm{d} \ln}{\mathrm{d}t} \frac{B^3}{n^2}$$

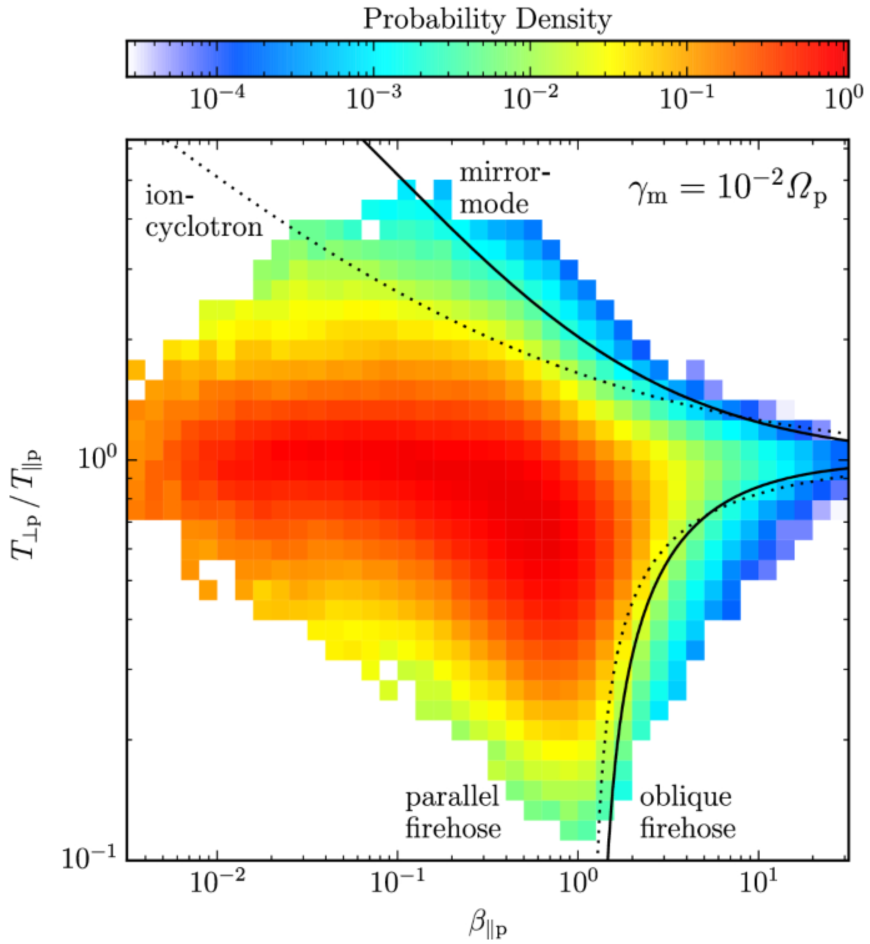

Solar wind distribution
[Verscharen+ 2019]

Minor-ion Heating in Solar Wind

Zhang+ from Squire *et al., 2022*

O^{5+} velocity distribution function (VDF)